Polym. Bull. (2015) 72:2809–2829
DOI 10.1007/s00289-015-1437-x

ORIGINAL PAPER

Aqueous radical polymerization of *N*,*N*-dimethylacrylamide redox-initiated by aerobically catalytic oxidation of water-soluble tertiary amines

Xiuting Wang[1] · Xiang Sun[1] · Guangqun Zhai[1,2]

Received: 12 November 2014 / Revised: 17 April 2015 / Accepted: 13 June 2015 /
Published online: 21 June 2015
© Springer-Verlag Berlin Heidelberg 2015

Abstract Catalytic oxidation of water-soluble tertiary amines by complexes of Cu^{II}, Fe^{III} and Co^{II} was utilized to initiate radical polymerization of *N*,*N*-dimethylacrylamide (DMAAm) in aqueous solution at 70–80 °C. The oxidation of tertiary amines by Cu^{II} was studied by proton nuclear magnetic resonance spectroscopy and online ultraviolet–visible spectrophotometry. The polymerization kinetics was monitored by gas chromatography, and molecular weight of the PDMAAm was measured by gel-permeation chromatography coupled with multi-angle laser light scattering. Oxidation of tertiary amines occurs predominantly via formation of C_{alpha}·radicals to initiate polymerization of electron-deficient monomers and *N*-dealkylation, and redox equilibrium between Cu^{I}/L and Cu^{II}/L is established at a faster rate in aqueous media. Fe^{III} and Cu^{II} complexes are efficient catalysts as each catalyst molecule could generate above 10 propagating radicals in 5 h, while Co^{II} complex might involve in oxidation of tertiary amines in non-radical pathway, leading to a low catalytic efficiency. Water-soluble tertiary amines such as *N*,*N*-dialkylethanolamine (alkyl = methyl, ethyl etc.) are reducing agents of a higher activity in aqueous media than those primary or secondary analogues. Our strategy renders it possible to prepare polymer of alpha-amino functionality via one-pot process from commercially available commodity reagents under practical conditions with negligible catalyst residue.

✉ Guangqun Zhai
zhai_gq@cczu.edu.cn

[1] Department of Materials Chemistry, College of Materials Science and Engineering, Changzhou University, Changzhou 213164, China

[2] Jiangsu Key Laboratory of Material Surface Science and Technology, School of Materials Science and Engineering, Changzhou University, Changzhou 213164, China

Keywords *N*,*N*-Dimethylacrylamide (DMAAm) · Aerobically catalytic oxidation · Radical polymerization · Tertiary amine · Alpha-amino functionality · Mono-centered redox-initiation

Introduction

It has been noted decades that oxidation of organic amines by peroxides involves formation of highly active radicals as intermediates, which initiate chain-growth polymerization of electron-deficient monomers such as (meth)acrylates, (meth)acrylamides, maleimides and acrylonitrile, leading to high-molecular-weight polymer [1, 2]. In most cases, peroxides oxidize amines via a radical mechanism, i.e. an electron transfer sequentially followed by proton transfer (ET-PT) [3–9] process. However, peroxides form dual-center initiation pairs with amines, i.e. each redox initiation pair generates one primary radical from a peroxide and another one from an amine, as shown in Scheme 1. As initiation efficiency and rate constants for propagation to monomers vary significantly among different primary radicals, it is anticipatable that such dual-center redox initiation leads to wide molecular-weight distribution (MWD) and polymer of heterogeneous terminal functionality. Therefore, a mono-centered redox-initiation technique might be the first step to prepare polymer of homogenous alpha-amino functionality.

Transition metal complexes in their super-normal or higher oxidation state could oxidize amines via a radical ET-PT mechanism, giving aminoalkyl radicals only to initiate polymerization. For instances, diperiodatocuprate anions in highly alkaline

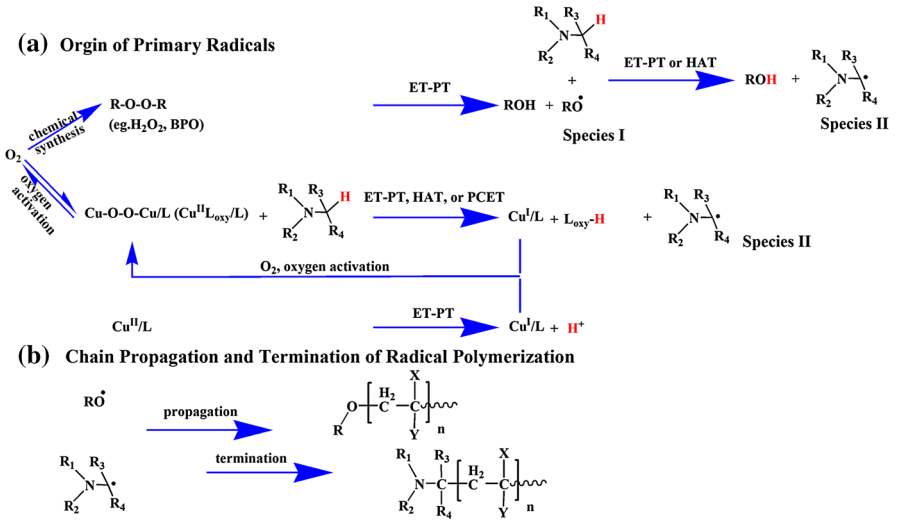

Scheme 1 **a** Origin of primary radicals by chemical oxidation of tertiary amines by peroxides and Cu^{II}/L complex, aerobically catalytic oxidation of tertiary amines; **b** Chain propagation and termination of radical polymerization of CH_2=CXY initiated by different primary radicals

media (Cu^{3+}/OH^{-}) oxidize amines to radicals to initiate polymerization, giving rise to Cu^{2+} as a by-product [10, 11]. Moreover, Cu^{2+} (Ref. [12–18]) and Ce^{4+} (Ref. [19–23]) could oxidize amines to aminoalkyl radicals, initiating polymerization under homogenous (in solutions or bulk) or heterogeneous (from surfaces) conditions, resulting in Cu^{+} and Ce^{3+}, respectively, as also illustrated in Scheme 1. Obviously, such a chemical oxidation technique makes it necessary to exploit a high dosage of transition metal cation complexes, which is typically considered as a major drawback.

Aerobic oxidation of tertiary amines under catalysis of transition metal cation complexes has been extensively investigated for decades. In general, transition metal salts in their lower oxidation state such as Fe^{II}, Cu^{I} and Co^{II} could steadily activate dioxygen (O_2) or hydroperoxide (H_2O_2) of lower oxidation activity by reversibly forming a series of highly oxidative complexes [24–33]. These oxidative complexes oxidize amines via radical mechanisms, including ET-PT, hydrogen atom transfer (HAT) and proton-coupled electron transfer (PCET) as well [34–37]. Only aminoalkyl radicals form to initiate polymerization, thus ensuring a homogenous alpha-amino functionality of final polymer. Furthermore, as O_2 binding by Fe^{II}, Cu^{I} and Co^{II} in a form of redox-active ligands, and the subsequent ligand release after a HAT or PT process with substrates are reversible even under aerobic media, a minimal amount of catalysts might be sufficient to achieve a pragmatic polymerization rate. Scheme 1 outlines the catalytic oxidation of amines as an initiation step for radical polymerization.

There have scarcely been any reports on catalytically redox-initiated radical polymerization. In the work on $CuSO_4$-hydrazine redox-initiated radical polymerization of methyl methacrylate (MMA) in the presence of O_2, Menon noticed that the polymerization still proceeded at 30 °C even with a $CuSO_4$ concentration at 1×10^{-5} mol L^{-1}. Therefore, the author proposed, after the reduction of Cu^{II} into Cu^{I} by hydrazine, Cu^{I} forms superoxo complex with O_2 (Cu^{II}–OO·), which abstracts a hydrogen atom (HAT) from hydrazine, leading to another N_2H_3· radical to initiate polymerization [38]. Thus, each Cu^{II} cation might generate multiple primary N_2H_3· radicals and PMMA chains during the polymerization. Recently, we reported that even a less than ppm-level dosage of $CuSO_4$ could trigger the self-initiated radical polymerization of 2-(*N*,*N*-dimethylamino)ethyl methacrylate in aqueous solutions at ambient temperature. Quantitative evaluation on the molecular weight results suggests that the turnover number (TON, defined as the number of propagating radicals per catalyst molecule) of Cu^{II} complexes could be more than 10^2 during the polymerization [39].

In this work, we examined the efficacy of such an initiation technique for radical polymerization of *N*,*N*-dimethylacrylamide (DMAAm) in aqueous solutions regarding the scope of amines, catalyst and redox-innocent ligands. Our results suggest even a ppm-level dosage of catalysts could successfully trigger the radical polymerization under aerobic media.

Experimental

Materials

N,*N*-Dimethylacrylamide (DMAAm >99.0 %), from Volant Chemical Co., Ltd., Nantong, China, was purified by passing through a column fitted with Na_2CO_3, nanosilica and basic Al_2O_3 (from top to bottom) to remove inhibitors and then stored in a refrigerator before use. Other materials were used as received. $CuCl_2{\cdot}2H_2O$ was from Xinbao Chemical Co., Ltd., Shanghai, China. Cobaltous acetate [$Co(OAc)_2$, >99.5 %] and 1,10-Phenanthroline hydrate (phen, >99.0 %) were from Runjie Chemical Co., Ltd., Shanghai, China. $CuSO_4{\cdot}5H_2O$, $FeCl_3$, Cobalt(II) acetylacetonate [$Co(acac)_2$, >97.0 %], Cobalt(III) acetylacetonate [$Co(acac)_3$, >98.0 %] and 2,2′-bipyridine (bPy, >99.0 %) were from Shanghai Chemical Reagent Co., Ltd., Shanghai, China. Ethylenediaminetetraacetic acid tetrasodium salt (EDTA, >99.0 %) was from Shanfeng Chemical Co., Ltd., Changzhou, China. *N*,*N*-Dimethylaminoethanol (DMAE, >99.0 %) was from Taihu Chemical Co., Ltd., Changzhou, China. Ethylenediamine (EDA, ≥99.5 %) was from Sinopharm Co., Ltd., Shanghai, China. *N*,*N*-Dimethylaniline (DMA, >99.0 %) and dimethylsulfoxide (DMSO, >99.0 %) were from Lingfeng Reagent Co., Ltd., Shanghai, China. *N*,*N*-Diethylaminoethanol (DEAE, >99.0 %) was from Nanxiang Reagents Co. Ltd., Shanghai, China. *N*,*N*-Diisopropylaminoethanol (DiPAE, >99.0 %) was from Xinde Environmental Sci & Technology Co. Ltd., Hangzhou, China. *N*,*N*,*N*′,*N*′-Tetramethylethylenediamine (TMEDA, ≥99.0 %) and *N*,*N*,*N*′,*N*′,*N*″-pentamethyldiethylenetriamine (PMDETA, ≥98.0 %) were from Jiangdian Chemical Co. Ltd., Changzhou, China. Tris(2-(*N*,*N*-dimethylamino)ethyl)amine (Me_6-TREN, >95 %) was purchased from Yipingtang Chemical Co., Ltd., Changzhou, China. *N*,*N*-Dimethylethylenediamine (DMEDA, ≥99.0 %) was purchased from Huadong Research Institute of Chemical Industry, Huaian, China. Branched poly(ethylene imine) (PEI, > 99 %, molecular weight ca. 10^4 g mol^{-1}) was from Alfa Aesar, Tianjin, China.

$CuSO_4$/bPy-DMAE redox process

0.5 mmol of $CuSO_4{\cdot}5H_2O$, 1.0 mmol of bPy, 5.0 mmol of DMAE and 5 mL of DMSO were added into a 50 mL single-necked round-bottom flask. The solution reacted at 70 °C for 40 h, and was exposed to air for O_2 diffusion for 2 min every 5 h. In another parallel experiment, 0.5 mmol of $CuCl_2{\cdot}2H_2O$/bPy complex was added. After the reaction, the supernatant was collected for nuclear resonance spectroscopic measurement.

Online monitoring of $CuSO_4$-amine redox process in the presence of O_2

$CuSO_4$-amine redox process in the presence of O_2 was online monitored by using temperature-regulated ultraviolet–visible (UV–Vis) spectroscopy. To prepare the solution, 0.1 mmol of $CuSO_4{\cdot}5H_2O$ and 0.2 mmol of bPy were added into 100 mL

of the DMAE/DMSO/water mixtures (v/v/v 50/0/50, 45/45/10, 0/50/50), 0.1 mmol of $CuSO_4 \cdot 5H_2O$ and 0.1 mmol of Me_6-TERN, PMDETA and TMEDA were added into 100 mL of the DMAE/water mixtures (v/v 50/50), respectively, and 0.05 mmol of $CuSO_4 \cdot 5H_2O$ and 0.01 mmol of phen were added into 100 mL of the DMAE/water mixtures (v/v 50/50). About 5 mL of solution was transferred to an Agilent Cary 100 UV–Vis spectrophotometer, and the cell temperature was set to 70 or 80 °C using a Varian dual-cell peltier accessory. The spectrum was collected periodically in a 15 min interval with the DMAE/DMSO/water solution as reference until no significant variance was observed.

Kinetic evaluation of UV–Vis spectrometric data

For the $CuSO_4$/bPy-DEAE redox process in the present of aerobic O_2, the first assumption was introduced such that Cu^{II}/bPy-amine and Cu^{I}/bPy-O_2 redox processes are first-order to the corresponding reactants. Thus,

$$\frac{\partial[\mathrm{Cu^I}]}{\partial t} = k_{\mathrm{ox}}[\mathrm{Cu^{II}}][\mathrm{Amine}] - k_{\mathrm{red}}[\mathrm{Cu^I}][\mathrm{O_2}] \tag{1}$$

in which $[Cu^I]$, $[Cu^{II}]$, [Amine] and $[O_2]$ are denoted as the corresponding concentration (mol L^{-1}), while k_{ox} and k_{red} represent the rate constants of Cu^{II}/bPy-amine and Cu^{I}/bPy-O_2 redox processes, respectively.

As the reacting media is open to air, the second assumption was introduced such that the concentration of Cu^{II} varies negligibly, while that of amine and O_2 maintain almost constant through the reaction. Thus, Eq. 1 can be transformed into the following Eq. 2:

$$\ln\left(1 - \frac{k_{\mathrm{red}}[\mathrm{O_2}]}{k_{\mathrm{ox}}[\mathrm{Cu^{II}}][\mathrm{Amine}]\varepsilon b}\ \mathrm{Abs.}\right) = -k_{\mathrm{red}}[\mathrm{O_2}]t \tag{2}$$

in which Abs. is the absorption of Cu^I/L, while ε and b represent the molar extinction coefficient of Cu^I/L complex (L mol^{-1} cm^{-1}) and distance of the UV–Vis cell (1 cm).

In general, k_{ox} and k_{red} are at a magnitude of order of 10^{-2} and 10^0 L mol^{-1} s^{-1} [40–42], ε of Cu^I/L is at a magnitude of order of 10^2–10^3 L mol^{-1} cm^{-1} [43–45], $[Cu^{II}]_0$ and $[amine]_0$ were fixed at 10^{-3} mol L^{-1} and 4.5–5.0 mol L^{-1} in this work; while $[O_2]$ at 70 °C is about 10^{-5} mol L^{-1} [46]. The factor $\frac{k_{\mathrm{red}}[\mathrm{O_2}]}{k_{\mathrm{ox}}[\mathrm{Cu^{II}}][\mathrm{Amine}]\varepsilon b}$ is estimated to be at a magnitude of order of 10^{-3}, and, as a result, the following approximation was adopted:

$$\ln\left(1 - \frac{k_{\mathrm{red}}[\mathrm{O_2}]}{k_{\mathrm{ox}}[\mathrm{Cu^{II}}][\mathrm{Amine}]\varepsilon b}\ \mathrm{Abs.}\right) = -\frac{k_{\mathrm{red}}[\mathrm{O_2}]}{k_{\mathrm{ox}}[\mathrm{Cu^{II}}][\mathrm{Amine}]\varepsilon b}\ \mathrm{Abs.} \tag{3}$$

As a consequence, Eq. 2 was transformed into the following one:

$$\mathrm{Abs.} = \left(k_{\mathrm{ox}}\left[\mathrm{Cu^{II}}\right][\mathrm{Amine}]\varepsilon b\right)t \tag{4}$$

Transition metal-amine redox-initiated radical polymerizations of DMAAm

10 mL of DMAAm and 10 mL of H_2O were added into a 50-mL round-bottom flask fitted with a stirring bar. About 1 mL of DMSO was added as the internal standard for the following gas chromatography (GC) measurement. A predetermined amount of the catalyst [viz. $FeCl_3$, $CuSO_4$, $Co(OAc)_2$, $Co(acac)_2$, or $Co(acac)_3$], ligand (viz. EDTA, TMEDA, or bPy, at a stoichiometric ratio of 2:1 to the catalyst; PMDETA, Me_6TREN, at a stoichiometric ratio of 1:1 to the catalyst) and the amine were added. An amine (DMA, DMAE, DEAE, DiPAE, EDA, DMEDA or PEI) was added to achieve a concentration of 10^{-3} or 10^{-2} mol L^{-1}, respectively. After the complete dissolution, the mixture was sealed to react in a preheated oil bath under mild stirring. After the aliquots were withdrawn at different time intervals, deionized water and hydroquinone were added quickly to dilute the solution and to quench the polymerization. For the polymer recovery, the reaction mixtures were dropped into the aqueous NaOH solutions at 70 °C, and the white gel [poly(*N*,N-dimethylacrylamide), PDMAAm] precipitated out due to the lower critical solution temperature (LCST)-type phase separation behavior [47]. The PDMAAm was collected and dried at 45 °C overnight. The details of the other parallel experiments are summarized in Table 1.

Estimation of catalyst efficiency

The catalytic efficiency was evaluated by turnover number (TON, defined as the number of propagating radicals per catalyst molecule), as estimated by using the following equations:

$$\mathrm{TON}_i = 1.10 \times \frac{[\mathrm{DMAAm}]_0 \times \mathrm{Conv.}_i \times \mathrm{MW}_{\mathrm{DMAAm}}}{\mathrm{MW}_{\mathrm{PDMAAm}} \times [\mathrm{Cu}^{\mathrm{II}}]_0}. \quad (5)$$

Table 1 Experimental details of transition metal-amine redox-initiated radical polymerizations of DMAAm

Series	Catalyst		Amine		Temp. (°C)
	Species	Amount (10^{-5} mol)	Species	Amount (10^{-3} mol)	
1	$CuSO_4$/bPy	1.0, 10.0	DiPAE	1.0	70, 80
2	$FeCl_3$/EDTA	0.1, 1.0, 2.5, 5.0, 10.0	DMAE	1.0	70, 80
			DEAE	1.0, 10.0	
			DiPAE	1.0, 10.0	
			DMA	1.0	
3	$Co(OAc)_2$/EDTA	1.0	DiPAE	1.0	70
4	$Co(acac)_2$/EDTA	1.0			
6	$CuCl_2$/bPy	1.0, 2.5, 5.0			70

Other conditions: 10 mL of H_2O, 10 mL of DMAAm, and 1 mL DMSO as the internal standard for GC measurement

In Eq. 5, $[DMAAm]_0$, $[Cu^{II}]_0$, MW_{DMAAm}, and MW_{PDMAAm} represent the initial concentration of DMAAm, initial concentration of catalyst, molar weight of DMAAm (99.13 g mol^{-1}), and molar weight of PDMAAm, while $Conv_{,i}$ stands for the corresponding monomer conversion at point *i*. The coefficient 1.10 was introduced to account for the fact that about 1.10 propagating PDMAAm radicals form one dead PDMAAm chain as disproportionation is the predominant termination of acrylamides [48–51].

Characterization

Monomer conversions were determined by GC using DMSO as an internal standard. Apparent number-average and weight-average molecular weights ($M_{n,GPC}$ and $M_{w,GPC}$) and polydispersity index (PDI $= M_{w,GPC}/M_{n,GPC}$) of polymers were determined by using a gel-permeation chromatography (GPC), which consisted of a Waters 515 isocratic HPLC pump, a Waters 2414 RI detector, a Waters Empower II software, a Waters 2707 autosampler and Waters columns (Styragel ⅂ HR 5, HR 4 and HR 3). The eluent was 0.07 mmol L^{-1} sodium nitrate DMF solution at 35 °C with a flow rate of 1 mL min^{-1} and the data were calibrated against linear PMMA standards. A Wyatt miniDAWN TRISTAR laser light scattering (LLS) detector and a Wyatt ViscoStar online viscometer were hyphenated with the GPC set-up to determine absolute weight-average MW ($M_{w,MALLS}$). LLS data were treated using Wyatt ASTRA software package ($dn/dc = 0.081$ mL g^{-1}) [51]. The UV–Vis spectrophotometry of the solution was performed on an Agilent Cary 100 UV–vis spectrophotometer, and cell temperature was fixed at 70 °C using a Varian dual-cell peltier accessory. Proton nuclear magnetic resonance (^{1}H-NMR) spectroscopy was performed on a Bruker DMX 500 M NMR spectrometer in $CDCl_3$ at room temperature, and the data were treated using MestRec software and calibrated against tetramethylsilane.

Results and discussion

$CuSO_4$-amine redox process

There have been different claims on chemical oxidation of aliphatic tertiary amines by transition metal complex in high oxidation state such as Cu^{II}/L or Fe^{III}/L, or aerobically catalyzed by transition metal complex in lower oxidation state [29, 52–59]. Scheme 2 summarizes the formation and subsequent transformation of primary intermediates involved in typical hypothetical routes of chemical oxidation or catalytic oxidation of DMAE using $CuSO_4$/bPy as a recyclable oxidizing agent, in situ bimolecular disproportionation to aminium and iminium, oxidative *N*-dealkylation to secondary or primary amines, proton transfer (PT) to C_{alpha}-H resulting in $C_{alpha}\cdot$ radicals. When it was added in another control experiment, $CuCl_2$/bPy is anticipated to play a dual of both an oxidizing agent to tertiary amines and a deactivator to $C_{alpha}\cdot$ radicals.

Figure 1 shows the ^{1}H-NMR spectra of the supernatant of $CuSO_4$/bPy-DMAE solution in DMSO after heating at 70 °C for 40 h. As there was no signal arising

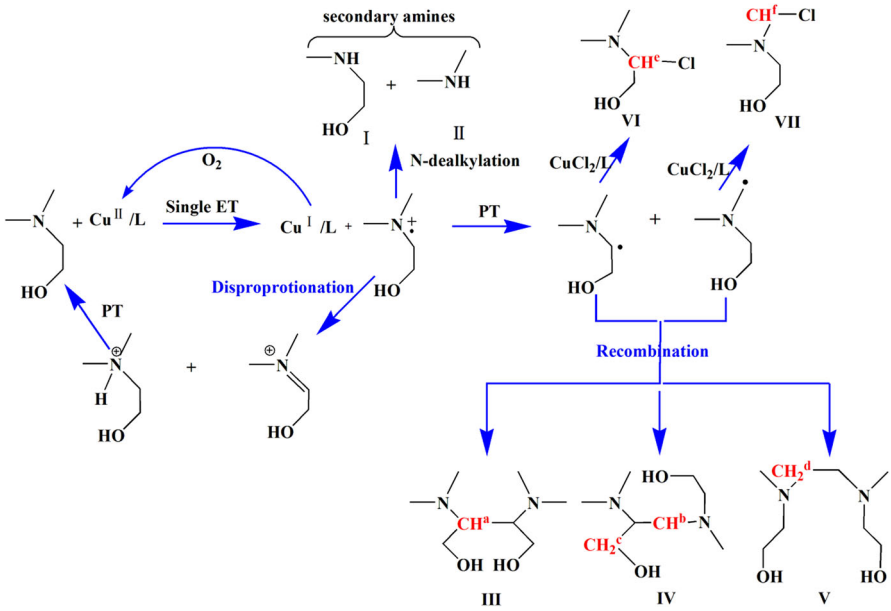

Scheme 2 Hypothetical routes of Cu^{II}/L-catalyzed oxidation of DMAE, structure and subsequent transformation of intermediates

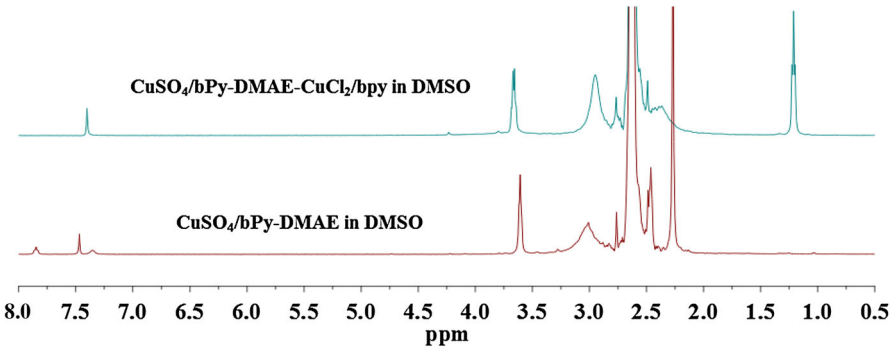

Fig. 1 ^{1}H-NMR spectra of the supernatant of (*bottom*) the $CuSO_4$/bPy-DMAE solution in DMSO and (*top*) the $CuSO_4$/bPy-DMAE-$CuCl_2$/bPy solution in DMSO after heating at 70 °C for 40 h

from unsaturated C***H*** (other than bPy), it seems that almost no imine or vinylidene moieties formed. Thus, the recombination (coupling) is the predominant termination over disproportionation for both aminium cation radicals and aminoalkyl radicals. The resonance peak at a chemical shift (δ) of 2.2–2.3 ppm was assigned to primary N-C_{alpha}-***H*** of DMAE and intermediates, that at 2.4–2.5 ppm was assigned to secondary N-C_{alpha}-***H*** moieties, such as C-$\boldsymbol{H_b}$ of species IV and C-$\boldsymbol{H_d}$ of species V, that at δ 2.7–2.8 ppm to C_{alpha}-***H*** of secondary amines (Species I and II, the intermediates derived from oxidative *N*-demethylation of DMAE), those at δ

2.9–3.1 ppm to tertiary N-C_{alpha}-$\boldsymbol{H_f}$ moieties of species V and alike. On the other hand, other *N*-dealkylated intermediates failed to be distinguishable due to overlap of the corresponding resonance signals. The intermediates derived from disproportionation of aminium radicals were not observed, in contrast to the postulation by Tang et al. [54, 60–62], while oxidative *N*-dealkylation (leading to secondary or primary amines) or PT to C_{alpha}-H (leading to aminoalkyl $C_{alpha}\cdot$ radicals) occur predominantly during Cu^{II}-tertiary amine redox process. Control experiment was performed in the presence of $CuCl_2$/bPy, but there is no peak at 4.5–4.7 ppm associating with primary or secondary N-C***H***-Cl moieties (species VI and VII), suggesting that $CuCl_2$/bPy might fail to work as a radical scavenger to deactivate $C_{alpha}\cdot$ radicals. A new peak at 1.23 ppm emerged and that at 2.27 ppm disappeared as a result of adding $CuCl_2$/bPy. A similar phenomenon was observed in Cu^{II}/L-catalyzed oxidation of DiPAE, although the specific mechanism kept uncertain.

As Cu^{II}/L could be reduced by amines to Cu^{I}/L, while Cu^{I}/L is in turn ready to aerobically oxidize to Cu^{II}/L, UV–Vis spectrophotometry was utilized to monitor the redox process. Figure 2a–c show the time-dependent UV–Vis absorption spectra

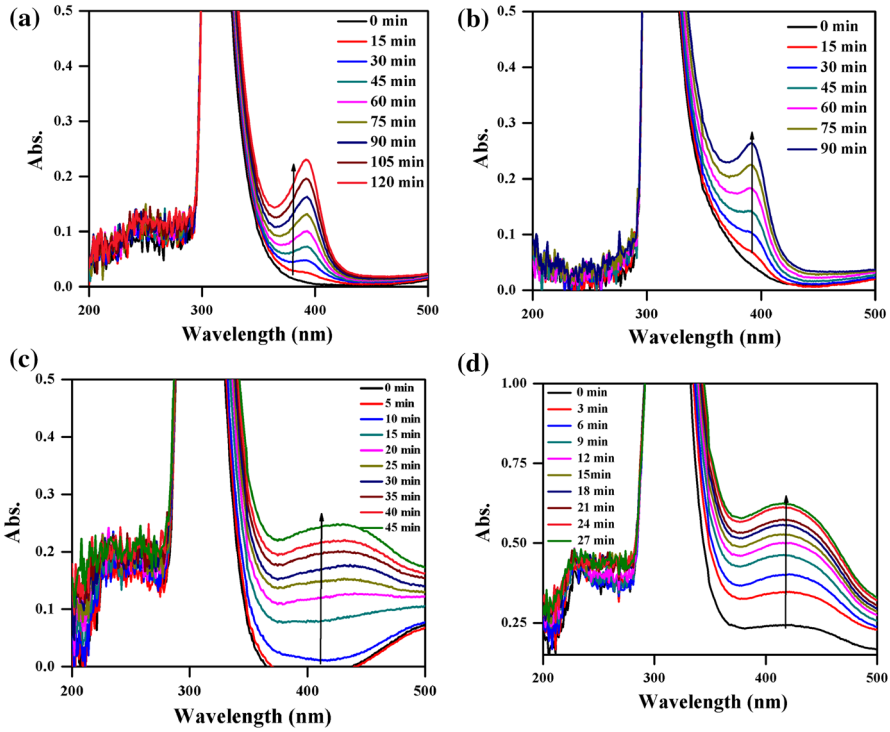

Fig. 2 Time-dependent UV–Vis absorption spectra over time of **a** the $CuSO_4$/bPy/DMAE/DMSO solution at 70 °C ($[CuSO_4/bPy]_0 = 10^{-3}$ mol L^{-1} in DMAE/DMSO (DMAE/H_2O/DMSO (v/v/v 50/0/50)); **b** the $CuSO_4$/bPy/DMAE/H_2O/DMSO solution at 70 °C ($[CuSO_4/bPy]_0 = 10^{-3}$ mol L^{-1} in DMAE/H_2O/DMSO (v/v/v 45/10/45)); **c** the $CuSO_4$/bPy/DMAE/H_2O solution at 70 °C ($[CuSO_4/bPy]_0 = 10^{-3}$ mol L^{-1} in DMAE/H_2O/DMSO (v/v/v 50/50/0)); **d** the $CuSO_4$/bPy/DMAE/H_2O solution at 80 °C ($[CuSO_4/bPy]_0 = 10^{-3}$ mol L^{-1} in DMAE/H_2O/DMSO (v/v/v 50/50/0))

of the $CuSO_4$/bPy-DMAE mixtures in different solvents at 70 °C. In common, a new absorption band appeared within the range of 370–430 nm, attributed to the formation and incremental accumulation of Cu^I/L. Figure 2d shows the time-dependent UV–Vis absorption spectra of the $CuSO_4$/bPy-DMAE mixtures in H_2O at 80 °C. Obviously, the absorption band associated with Cu^I/bPy became increasingly intense in a much higher rate than 70 °C, suggesting a faster oxidation of tertiary amines by Cu^{II}/bPy at elevated temperature.

Figure 3 shows the Abs.–time profiles and linear fitting by using Eq. 4 of the $CuSO_4$/bPy-DMAE pairs in different media, as derived from Fig. 2, respectively. As the slope of the fit lines is directly proportional to the rate constant for Cu^{II}/bPy-DMAE redox process (k_{ox}), it is inferred that the Cu^{II}/bPy-DMAE redox process proceeds in a faster rate in aqueous media than in DMSO. The fitting derived from the UV–Vis data of the $CuSO_4$/bPy-DMAE in water at 80 °C (Fig. 2d) gave rise to less linearity, which indicates a very faster redox rate of both Cu^{II}/bPy-DMAE process and Cu^I/bPy-O_2 process.

The effect of ligands on the Cu^{II}-DMAE redox process was briefly examined. When a multi-dentate tertiary amine including TMEDA, PMDETA or Me_6TERN was used as the ligand, only a marginal absorption band associated with Cu^I species was observed even at 80 °C, as shown in Fig. 4a, indicating a very low cumulative concentration of Cu^I species. However, as expressed by in Eq. 1, a low [Cu^I] might be ascribed to a low k_{ox} for Cu^{2+}-amine redox process or a higher k_{red} for Cu^+-O_2 redox process. Nonetheless, when phen was used as the ligand, as shown in Fig. 4b, Cu^I/L species accumulated at a much faster rate than when bPy used as the ligand, indicating a high k_{ox} for Cu^{2+}/phen-amine redox process or a lower k_{red} for Cu^+/phen-O_2 redox process. A high half-wave electrochemical potential reflects a low reduction ability of Cu^I complexes. The half-wave potential of Cu^I/bPy, Cu^I/

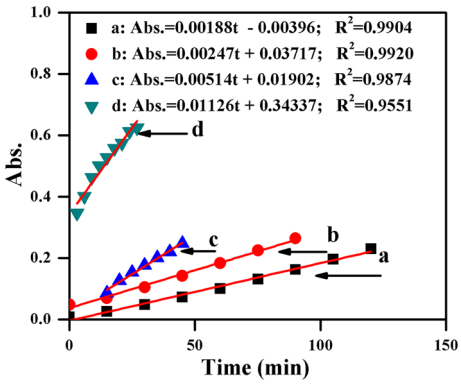

Fig. 3 Abs.–time profiles of the Cu^I/bPy species in the $CuSO_4$/bPy-DMAE in different media, and linear fitting by using Eq. 4 as derived from Fig. 2. *a* The $CuSO_4$/bPy/DMAE/DMSO solution at 70 °C ($[CuSO_4/bPy]_0 = 10^{-3}$ mol L^{-1} in DMAE/DMSO (v/v/v 50/0/50); *b* the $CuSO_4$/bPy/DMAE/H_2O/DMSO solution at 70 °C ($[CuSO_4/bPy]_0 = 10^{-3}$ mol L^{-1} in DMAE/H_2O/DMSO (v/v/v 45/10/45)); *c* the $CuSO_4$/bPy/DMAE/H_2O solution at 70 °C ($[CuSO_4/bPy]_0 = 10^{-3}$ mol L^{-1} in DMAE/H_2O/DMSO (v/v/v 50/50/0)); *d* the $CuSO_4$/bPy/DMAE/H_2O solution at 80 °C ($[CuSO_4/bPy]_0 = 10^{-3}$ mol L^{-1} in DMAE/H_2O/DMSO (v/v/v 50/50/0))

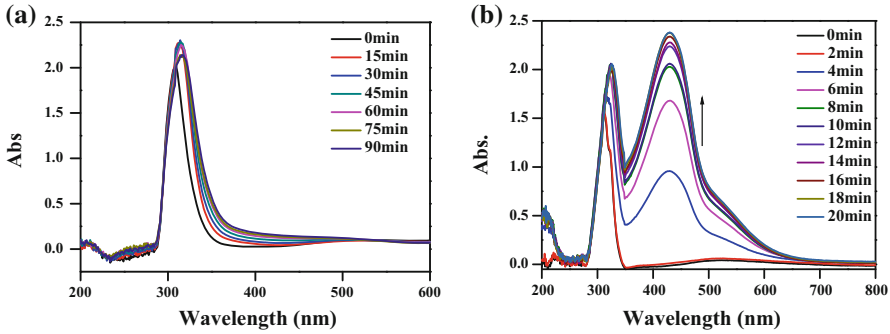

Fig. 4 Time-dependent UV–Vis absorption spectra of **a** the $CuSO_4/Me_6$-TERN/DMAE/H_2O solution at 80 °C, $[CuSO_4/Me_6\text{-TERN}]_0 = 10^{-3}$ mol L^{-1} in DMAE/H_2O (v/v 50/50); **b** the $CuSO_4$/phen/DMAE/H_2O solution at 80 °C, $[CuSO_4/\text{phen}]_0 = 5 \times 10^{-4}$ mol L^{-1} in DMAE/H_2O(v/v 50/50)

PMDETA and Cu^I/Me_6-TREN complexes in acetonitrile has been determined to be −0.421 mV, −0.489 mV ($\Delta E_p = 65$ mV), −0.717 mV ($\Delta E_p = 71$ mV), respectively [63, 64]. It suggests that Cu^I/bPy exhibits a superior stability to Cu^I/PMDETA and Cu^I/Me_6-TREN. Besides, Coullerez et al. reported that *N*,*N*-dimethylamino moieties of ligands would enhance the stability of the Cu^{II} complex [64]. Thus, Cu^{II}/bPy or Cu^{II}/phen complexes exhibit a higher oxidation activity than Cu^{II}/TMEDA Cu^{II}/PMDETA and Cu^{II}/Me_6-TREN.

Radical polymerization of DMAAm redox-initiated by aerobically catalytic oxidation of tertiary amines

Several different metal/ligand complexes were attempted by using DiPAE as the reducing agent to initiate radical polymerization of DMAAm, including $FeCl_3$/EDTA, $CuSO_4$/bPy, $Co(OAc)_2$/EDTA, $Co(acac)_2$/EDTA and $Co(acac)_3$/EDTA. It was surprising that $Co(acac)_3$/EDTA, albeit in higher oxidation state, could not trigger the polymerization, while both $Co(OAc)_2$/EDTA and $Co(acac)_2$/EDTA successfully catalyzed the polymerization. It might suggest that Co^{II} forms Co^{IV}-oxo complex [65], rather than Co^{III}-peroxo complexes, as illustrated in Scheme 3.

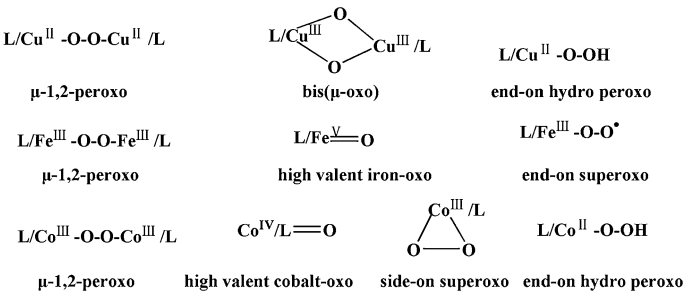

Scheme 3 Structure and nomenclature of water-soluble oxidative complexes of Cu, Fe and Co cations

Figure 5 shows the conversion–time profiles of the radical polymerization of DMAAm at 70 °C redox-initiated by the pairs of DiPAE with $Co(OAc)_2$/EDTA and $Co(acac)_2$/EDTA ($[Co^{II}]_0$:$[DiPAE]_0 = 1:10^2$), respectively. In both cases, no induction took place during the polymerization even in the presence of O_2. The conversion reached about 62 % in 25 min and gradually leveled off due to the glassy state effect for the polymerization using $Co(acac)_2$/EDTA. On the other hand, the conversion reached about 40 % in 25 min and increased to about 80 % in 245 min for the polymerization using $Co(OAc)_2$/EDTA. The catalytic efficiency of Co^{II} was evaluated by turnover number (TON), denoting as the number of propagating radicals per catalyst molecule, which was estimated by using Eq. 5. MW and PDI of the PDMAAm sample were measured by GPC-MALLS. The relative number-average molecular weight ($M_{n,GPC}$) and PDI were determined to be 2.25×10^5 g mol^{-1} and 1.91 by GPC against PMMA standards. The absolute weight-average molecular weight ($M_{W,MALLS}$) was determined to be 7.72×10^5 g mol^{-1} by MALLS, as shown in Fig. 6. Similar to most typical conventional radical polymerization, there is no control on molecular weight and its distribution. It was deemed that the average molecular weight of PDMAAm varied les remarkably, and the molecular weight distribution remained broad through the entire processes. $M_{W,MALLS}$ was used in evaluating TON. Figure 5 compares the variation of TON of Co^{II} with the reaction time. Obviously, each Co^{II} molecule appeared to generate about 1.0–2.0 propagating radicals within 4 h. It indicates that although the polymerization rate was rather rapid, the catalytic efficiency was somehow low, and almost no catalyst regeneration occurred.

In the presence of O_2 or H_2O_2, transition metal cations in their lower oxidation state could form oxidative complexes of different stoichiometric ratio and configuration under proper conditions. Representative water-tolerant oxidative

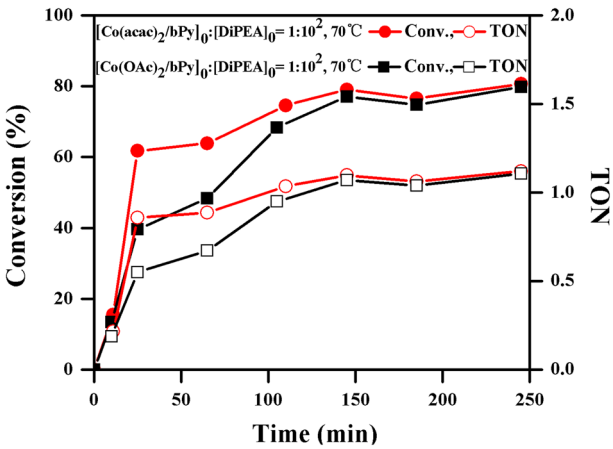

Fig. 5 Conversion–time profiles and the catalyst efficiency (TON) of the radical polymerization of DMAAm redox-initiated by $Co(acac)_2$/bPy-DiPAE pair and $Co(OAc)_2$/bPy-DiPAE pair; reaction conditions: 10^{-5} mol of $Co(acac)_2$/bPy or $Co(OAc)_2$/bPy, 10^{-3} mol of DiPAE, in 20 mL of DMAAm/H_2O mixture (v/v 50/50), 70 °C

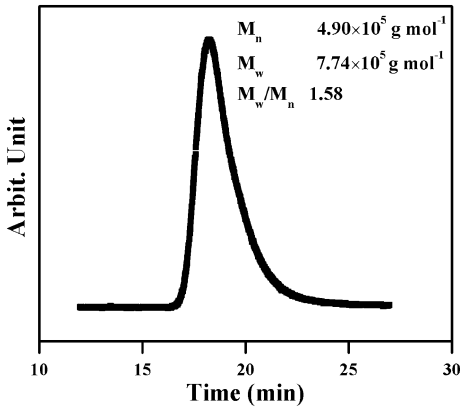

Fig. 6 Chromatogram trace of the PDMAAm sample by GPC-MALLS using DMF as the mobile phase. PDMAAm sample was prepared via the polymerization redox-initiated by $CuSO_4$/bPy-DiPAE pair at 80 °C

complexes of Cu [66–68], Fe [69–71] and Co [72, 73] are listed in Scheme 3. If Co^{II} is a redox catalyst of a sufficiently high activity as anticipated, even a minimal concentration of Co^{II} might still work well to trigger the polymerization. However, no polymerization would occur if the $[Co^{II}]_0$:$[DiPAE]_0$ feed ratio was further reduced to 1:10^3 even at 80 °C. This fact might arise from the formation of oxidative complexes under different stoichiometric ratios of Co^{II} to O_2, which might oxidize tertiary amines in non-radical pathways.

The control experiments were performed by using $CuSO_4$/bPy and $FeCl_3$/EDTA as the catalyst. Figure 7 shows the time-conversion profiles of the radical polymerization of DMAAm redox-initiated by $CuSO_4$/bPy–DiPEA and $FeCl_3$/EDTA pairs ($[catalyst]_0$:$[DiPAE]_0$ = 1:10^2) at 70 °C and corresponding TON

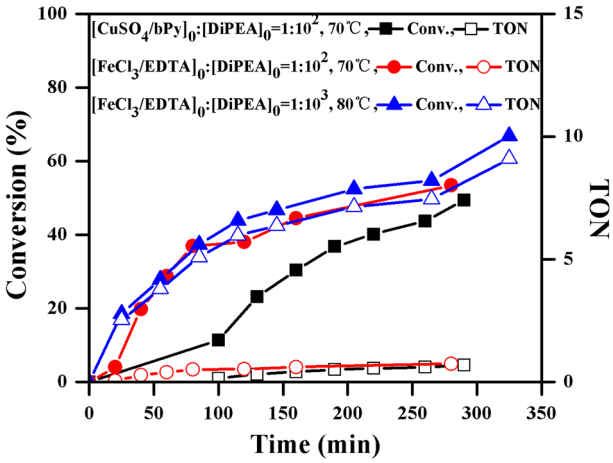

Fig. 7 Conversion–time profiles and the catalyst efficiency (TON) of the radical polymerization of DMAAm redox-initiated by $CuSO_4$/bPy-DiPAE pair or $FeCl_3$/EDTA-DiPAE pair; reaction conditions: 10^{-6} or 10^{-5} mol of $CuSO_4$/bPy or $FeCl_3$/EDTA, 10^{-3} mol of DiPAE, in 20 mL of DMAAm/H_2O mixture (v/v 50/50), 70 or 80 °C

variation of the catalyst during the polymerization. Clearly, the polymerization was successfully catalyzed by either $CuSO_4$/bPy or $FeCl_3$/EDTA, but it reached a conversion of DMAAm less than 60 % even within 5 h, much slower than that by $Co(OAc)_2$/EDTA or $Co(acac)_2$/EDTA. The catalytic efficiency was rather low, as shown in Fig. 7. Similarly, a lower feed concentration of $CuSO_4$/bPy and $FeCl_3$/EDTA cannot trigger the polymerization at 70 °C. The parallel experiments were conducted at 80 °C. Figure 7 shows the kinetic profiles of the radical polymerization of DMAAm redox-initiated by a $FeCl_3$/EDTA–DiPEA pair ($[FeCl_3/EDTA]_0$:$[DiPAE]_0 = 1{:}10^3$) at 80 °C and corresponding TON variation of the catalyst during the polymerization. Obviously, the process underwent in a much faster rate, and a higher TON than that at 70 °C, respectively, indicating a high energy of activation (ΔE_a) of such a catalytic redox initiation. The polymerization using a $[FeCl_3/EDTA]_0$:$[DiPAE]_0$ molar feed ratio of $1{:}10^4$ was also performed, but no remarkable viscosification took place within several hours. On the other hand, as shown in Fig. 8, the polymerization redox-initiated by a $CuSO_4$/bPy–DiPEA pair ($[CuSO_4/bPy]_0$:$[DiPAE]_0 = 1{:}10^2$) at 80 °C proceeded at a comparable rate to that at 70 °C, For example, it reached a conversion of about 10 % in 20 min, 46 % in 80 min and 64 % in 340 min, respectively, suggesting the $CuSO_4$/bPy–DiPEA pairs might exhibit a low ΔE_a. The polymerization redox-initiated by a $CuSO_4$/bPy–DiPEA pair ($[CuSO_4/bPy]_0$:$[DiPAE]_0 = 1{:}10^3$) proceeded at a slower rate, as it achieved a conversion of about 25 % in 50 min, 42 % in 50 min and 50 % in 340 min. However, Fig. 8 shows that the latter ($[CuSO_4/bPy]_0$:$[DiPAE]_0 = 1{:}10^3$) exhibited a higher catalytic efficiency than the former ($[CuSO_4/bPy]_0$:$[DiPAE]_0 = 1{:}10^2$), as TON of $CuSO_4$/bPy increased to about 6.35 and 0.80, respectively. The polymerization using a $[CuSO_4/bPy]_0$:$[DiPAE]_0$ molar feed ratio of $1{:}10^4$ was also performed. However, the polymerization underwent so slowly that the conversion was less than 5 % within 5 h.

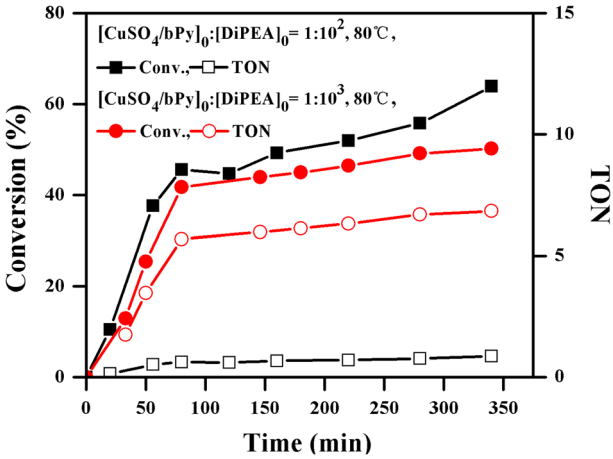

Fig. 8 Conversion–time profiles and the catalyst efficiency (TON) of the radical polymerization of DMAAm redox-initiated by $CuSO_4$/bPy-DiPAE pair; reaction conditions: 10^{-6} or 10^{-5} mol of $CuSO_4$/bPy, 10^{-3} mol of DiPAE, in 20 mL of DMAAm/H_2O mixture (v/v 50/50), 80 °C

The effect of counterions to transition metal cations was briefly studied by using $CuCl_2$/bPy as the catalyst. Figure 9 shows the kinetic profiles of the radical polymerization of DMAAm redox-initiated by $CuCl_2$/bPy–DiPEA pairs ([$CuCl_2$/bPy]$_0$:[DiPEA]$_0$ = 1:10^2, 2.5:10^2 and 5:10^2, respectively). Different from the analogues using $CuSO_4$/bPy as the catalyst, the polymerization using $CuCl_2$/bPy exhibited a complicated rate dependence on the concentration of $CuCl_2$/bPy. In particular, the polymerization rate increased initially with an increasing catalyst concentration ([$CuCl_2$/bPy]$_0$:[DiPEA]$_0$ feed ratio from 1:10^2 to 2.5:10^2), but adversely decreased with the further increase in the catalyst concentration ([$CuCl_2$/bPy]$_0$:[DiPEA]$_0$ feed ratio from 2.5:10^2 to 5.0:10^2). Such an unusual behavior was attributed to the dual role of $CuCl_2$/bPy complexes as both an oxidizing agent to generate primary radicals and a radical scavenger as the deactivation step in atom transfer radical polymerization. Similarly, as shown in Fig. 10, when $FeCl_3$/EDTA used as the catalyst, the dual role of $FeCl_3$/EDTA complexes resulted in a comparable rate dependence on the catalyst concentration. In other words, when the transition metal cations with (pseudo)halides (M^nX_n, M=Co, Fe, Cu, Ni; X=Cl^-, Br^-, I^-, or $(CH_3CH_2)_2NC(=S)S^-$) as the counterions, the catalyst concentration has to be optimized by taking the radical deactivation into account. Otherwise, efficient retardation or inhibition might occur in the presence of a high concentration of inhibitive oxidizing agents.

The effect of amines on the polymerization was also studied. In general, the primary or secondary amines, such as EDA, DMEDA or PEI, exhibit a very low activity in redox-initiating radical polymerization of DMAAm using either Cu^{II}, Co^{II} or Fe^{III} as the catalyst, probably due to the oxidation in non-radical pathways. As typical tertiary amines such as triethylamine are sparely water-soluble, very limited conversion of DMAAm was observed when using them as a reducing agent. Besides, although the polymerization using *N*,*N*-dimethylaniline (DMA) as the reducing agent steadily reached a high conversion of above 50 % in 5 h, the thermally induced DMA-initiated radical polymerization cannot be excluded from redox-initiated radical one [74, 75].Thus, DMA was opted out as the substrate for catalytic oxidation for radical polymerization of DMAAm. Effort was concentrated on water-soluble tertiary amines, such as DMAE and DEAE. Figure 11 shows the

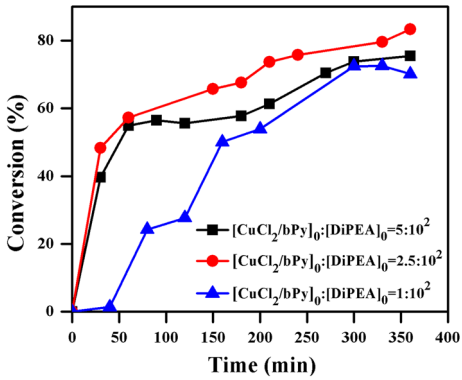

Fig. 9 Conversion–time profiles of the radical polymerization of DMAAm redox-initiated by $CuCl_2$/bPy-DiPAE pair; reaction conditions: 10^{-5}, 2.5 × 10^{-5}, 5.0 × 10^{-5} mol of $CuCl_2$/bPy, 10^{-3} mol of DiPAE, in 20 mL of DMAAm/H_2O mixture (v/v 50/50), 70 °C

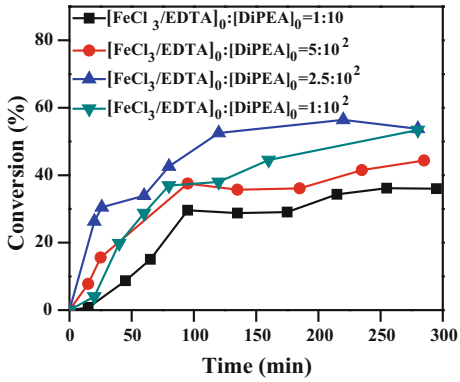

Fig. 10 Conversion–time profiles of the radical polymerization of DMAAm redox-initiated by $FeCl_3$/EDTA-DiPAE pair; reaction conditions: 10^{-5}, 2.5×10^{-5}, 5.0×10^{-5}, 1.0×10^{-4} mol of $FeCl_3$/EDTA, 10^{-3} mol of DiPAE, in 20 mL of DMAAm/H_2O mixture (v/v 50/50), 70 °C

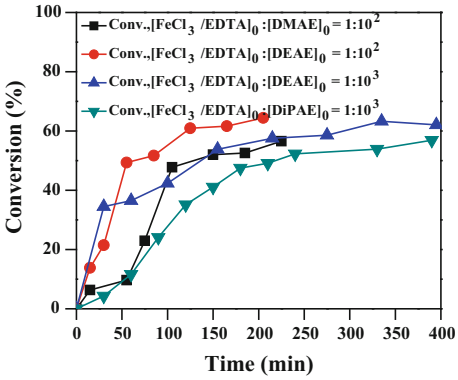

Fig. 11 Conversion–time profiles of the radical polymerization of DMAAm redox-initiated by $FeCl_3$/EDTA-DMAE, $FeCl_3$/EDTA-DEAE and $FeCl_3$/EDTA-DiPAE pair; reaction conditions: 10^{-5} mol of $FeCl_3$/EDTA, 10^{-3} mol of DMAE or DEAE (for $[FeCl_3/EDTA]_0$:$[Amine]_0 = 1:10^2$), or 10^{-2} mol of DEAE or DiPAE (for $[FeCl_3/EDTA]_0$:$[Amine]_0 = 1:10^3$), in 20 mL of DMAAm/H_2O mixture (v/v 50/50), 70 °C

kinetic profiles of the radical polymerization of DMAAm redox-initiated by pairs of $FeCl_3$/EDTA complex with DMAE, DEAE and DiPAE at different molar feed ratio. Generally, the polymerization redox-initiated by $FeCl_3$/EDTA-DEAE exhibited a faster rate than those by $FeCl_3$/EDTA-DMAE or $FeCl_3$/EDTA-D*i*PEAE under similar reaction conditions. In addition, when $CuSO_4$/bPy-tri(ethanol)amine (TEAA) was used at 70 °C, the polymerization reached a conversion of about 7–8 % in 2 h. Thus, it is inferred that *N*,*N*-dialkylaminoethanol of labile C_{alpha}-H moieties, e.g. DMAE, DEAE and DiPAE etc., might be the suitable candidate for the catalytic aerobic oxidation by transition metal cation complexes for radical polymerization of DMAAm in aqueous media.

The effect of ligands on the polymerization was briefly compared. The polymerization could not occur in the absence of any multidentate ligands, as proper ligands not only protect Cu^{II}/Fe^{III}/Co^{II} from hydrolysis and precipitation, but

also regulate redox potentials against O_2 or amines, and enhance the redox-initiation rate as well. However, EDTA appears to be the only ligand with $FeCl_3$ to successfully trigger the polymerization, while bPy and Phen are suitable ligands to Cu^{II}. The complexes of Cu^{II} or Fe^{III} with typical multi-dentate tertiary amines, such as TMEDA, PMDETA and Me_6TREN, seem to be of a very low activity in catalyzing such a process, suggesting a low k_{ox} for Cu^{2+}-amine redox process.

As the residue of tertiary amines, the alpha-amino functionality of PDMAAm afford further functionalization, such as using as a macro-sensitizer for UV-induced diarylketone-initiated radical polymerization to prepare block copolymer. As a mono-centered redox-initiation mechanism, our protocol affords the one-pot preparation of polymer of 100 % alpha-amino functionality from commercially available and commodity reagents under less demanding conditions (viz., ionic or controlled radical polymerization, or post-polymerization end-group modification). The pursuit of catalysts of high activity could further reduce the catalyst concentration without sacrificing polymerization rate. Our strategy might also be applicable to heterogeneous processes, such as radical polymerization in aqueous emulsion, which is undertaken and would be presented in a separate report.

Conclusion

The aerobic oxidation of water-soluble tertiary amines under the catalysis of the complexes of $Co^{II,}$ Fe^{III} and Cu^{II} with multi-dentate ligands ($[catalyst]_0$:$[amine]_0$ $\leq 1:10^2$) was attempted to initiate radical polymerization of *N*,*N*-dimethylacrylamide (DMAAm) in aqueous solutions at 70–80 °C. When used in conjunction with DiPAE, the complexes of Fe^{III} and Cu^{II} exhibit a high catalytic efficiency than that of Co^{II}, as the former could generate more than several to ten propagating radicals within 5 h. Water-soluble tertiary amines of labile C_{alpha}-H moieties, e.g. *N*,*N*-dialkylethanolamine (alkyl = methyl, ethyl etc.), exhibit an enhanced activity over those primary or secondary amines or triethanolamine as the substrate (reducing agents) in such a aerobically catalytic oxidation for radical polymerization. Our protocol affords the one-pot preparation of polymer of 100 % alpha-amino functionality from commercially available commodity reagents via a mono-centered redox-initiation mechanism under less demanding conditions.

Acknowledgments This work was supported by the Natural Science Foundation of China (21174020, 21474010), a Project Funded by the Priority Academic Program Development of Jiangsu Higher Education Institutions.

References

1. Misra GS, Bajpai UND (1982) Redox polymerization. Prog Polym Sci 8:61–131
2. Sarac AS (1999) Redox polymerization. Prog Polym Sci 24:149–1204. doi:10.1016/S0079-6700(99)00026-X
3. Sideridou ID, Achilias DS, Karava O (2006) Reactivity of benzoyl peroxide/amine system as an initiator for the free radical polymerization of dental and orthopaedic dimethacrylate monomers:

effect of the amine and monomer chemical structure. Macromolecules 39:2072–2080. doi:10.1021/ma0521351
4. Sato T, Kita S, Otsu T (1975) A study on initiation of vinyl polymerization with diacyl peroxide-tertiary amine systems by spin trapping technique. Makromol Chem 176:561–571. doi:10.1002/macp.1975.021760303
5. Feng XD (1986) Role of aminium radical in the initiation of vinyl polymerization. Chin J Polym Sci 4:109–118
6. Feng XD, Guo XQ, Qiu KY (1988) Study of the initiation mechanism of the vinyl polymerization with the system persulfate/*N*, *N*, *N*′, *N*′-tetramethylethylenediamine. Makromol Chem 189:77–83. doi:10.1002/macp.1988.021890108
7. Achilias DS, Sideridou ID (2004) Kinetics of the benzoyl peroxide/amine initiated free-radical polymerization of dental dimethacrylate monomers: experimental studies and mathematical modeling for TEGDMA and Bis-EMA. Macromolecules 37:4254–4265. doi:10.1021/ma049803n
8. Qiu KY (2008) Development of radical polymerization in recent twenty years. Chin Polym Bull 7:15–28
9. Feng XD, Qiu KY (2005) Radical polymerization in the presence of amine and living radical polymerization. Chin Polym Bull 4:23–34
10. Deng KL, Liu J, Wang GZ, Tian H, Ren XB, Zhong HB, Zhang PF (2008) Potassium diperiodatocuprate-mediated preparation of poly (methyl methacrylate)/organo-montmorillonite composites via in situ grafting copolymerization. Express Polym Lett 2:677–686. doi:10.3144/expresspolymlett.2008.80
11. Liu YH, Shang YJ, Li WP, Wang Z, Deng KL (2000) Study on the kinetics of acrylonitrile polymerization initiated by diperiodatonickelate(IV) periodate complex. Acta Polym Sin 2:235–238
12. Sumalekshmy S, Gopidas KR (2005) Reaction of aromatic amines with $Cu(ClO_4)_2$ in acetonitrile as a facile route to amine radical cation generation. Chem Phys Lett 413:294–299. doi:10.1016/j.cplett.2005.06.041
13. Yao RR, Wu R, Zhai GQ (2014) Direct grafting poly(methyl methacrylate) from TiO_2 nanoparticles via Cu^{2+}-amine redox-initiated radical polymerization: an advantage of mono-center initiation. Polym Sci Eng. doi:10.1002/pen.23939 **(In press)**
14. Chen XB, Zhai GQ (2012) $CuSO_4$-amine redoxinitiated graft polymerization from glass substrate surface. Acta Polym Sin 1295–1306
15. Chen XB, Zhai GQ (2014) Facile preparation of SiO_2 hybrid nanoparticles via Cu^{2+}-amine redox-initiated radical polymerization. Polym Bull 71:1291–2610. doi:10.1007/s00289-014-1209-z
16. Tao F, Chen XB, Zhai GQ (2013) Stimuli-responsive SiO_2-graft-poly(sodium acrylate) hybrid nanoparticles via Cu^{2+}-amine redox-initiated radical polymerization. Macromol Chem Phys 214:2792–2801. doi:10.1002/macp.201300455
17. Gao J, Song W, Wang P, Zhai GQ (2014) $CuSO_4$-amine redox-initiated radical polymerization of methyl methacrylate mediated by a $CuCl_2$ complex: homogeneous reverse ATRP. J Polym Sci Polym Chem 52:2562–2578. doi:10.1002/pola.27272
18. Wu R, Zhai GQ (2013) One-pot facile preparation of TiO_2-graft-poly(methyl methacrylate) hybrid nanoparticles via Cu^{2+}-amine redox initiated radical polymerization. Acta Polym Sin 191–198
19. Tsubokawa N, Maruyama K, Sone Y, Shimomura M (1989) Graft polymerization of acrylamide from ultrafine silica particles by use of a redox system consisting of ceric ion and reducing groups on the surface. Polym J 21:475–481. doi:10.1295/polymj.21.475
20. Abdollahi M, Rouhani M, Hemmati M, Salarizadeh P (2013) Grafting of water-soluble sulfonated monomers onto functionalized fumed silica nanoparticles via surface-initiated redox polymerization in aqueous medium. Polym Int 62:713–720. doi:10.1002/pi.4351
21. Peng M, Liao ZJ, Zhu ZM, Guo HL, Wang HJ (2009) Fumed silica/polymer hybrid nanoparticles prepared by redox-initiated graft polymerization in emulsions. J Mater Sci 44:6286–6293. doi:10.1007/s10853-009-3865-1
22. Abdollahi M, Rouhani M (2012) Hydrophilic polymer/fumed silica hybrid nanoparticles synthesized via surface-initiated redox polymerization. J Polym Res 19:1–10. doi:10.1007/s10965-012-0005-4
23. Abdollahi M, Salarizadeh P, Rouhani M, Rekabdar F (2014) Grafting of hydrophilic monomers onto aminopropyl-functionalized sodium montmorillonite via surface-initiated redox polymerization. Polym Int 63:576–583. doi:10.1002/pi.4593
24. Cho J, Sarangi R, Nam W (2012) Mononuclear metal-O_2 complexes bearing macrocyclic *N*-tetramethylated cyclam ligands. Acc Chem Res 45:1321–1330. doi:10.1021/ar3000019

25. Kitajima N, Moro-oka Y (1994) Copper–dioxygen complexes. inorganic and bioinorganic perspectives. Chem Rev 94:737–757. doi:10.1021/cr00027a010
26. Decker A, Solomon EI (2005) Dioxygen activation by copper, heme and non-heme iron enzymes: comparison of electronic structures and reactivities. Curr Opin Chem Biol 9:152–163. doi:10.1016/j.cbpa.2005.02.012
27. Lewis EA, Tolman WB (2004) Reactivity of dioxygen–copper systems. Chem Rev 104:1047–1107. doi:10.1021/cr020633r
28. Solomon EI, Wong SD, Liu LV, Decker A, Chow MS (2009) Peroxo and oxo intermediates in mononuclear nonheme iron enzymes and related active sites. Curr Opin Chem Biol 13:99–113. doi:10.1016/j.cbpa.2009.02.011
29. Chiavarino B, Cipollini R, Crestoni ME, Fornarini S, Lanucara F, Lapi A (2008) Probing the compound I-like reactivity of a bare high-valent oxo iron porphyrin complex: the oxidation of tertiary amines. J Am Chem Soc 130:3208–3217. doi:10.1021/ja077286t
30. Koveleva EG, Neibergall MB, Chakrabarty S, Lipscomb JD (2007) Finding intermediates in the O_2 activation pathways of non-heme iron oxygenases. Acc Chem Res 40:475–483. doi:10.1021/ar700052v
31. Drago RS, Stahlbush JR, Kitko DJ, Breese J (1980) Five-coordinate dioxygen adducts of cobalt(II) complexes. J Am Chem Soc 102:1884–1889. doi:10.1021/ja00526a021
32. Eaton RD, O'Reilly A (1987) Oxidation of cobalt(II) amine complexes to mononuclear cobalt (III) complexes by dioxygen. Inorg Chem 26:4185–4188. doi:10.1021/ic00272a010
33. Kurahashi T, Fujii H (2013) Unique ligand-radical character of an activated cobalt salen catalyst that is generated by aerobic oxidation of a cobalt(II) salen complex. Inorg Chem 52:3908–3919. doi:10.1021/ic302677f
34. Tkatchouk E, Fomina L, Rumsh L, Fomine S (2003) Role of (μ-oxo)dicopper(III) complexes in oxidative polymerization of phenol. A DFT study. Macromolecules 36:5607–5612. doi:10.1021/ma0342731
35. Evans S, Smith JRL (2001) The oxidation of ethylbenzene by dioxygen catalysed by supported iron porphyrins derived from iron(III) tetrakis(pentafluorophenyl)-porphyrin. J Chem Soc Perkin Trans 2:174–180. doi:10.1039/B007326L
36. Lyaskovskyy V, Suarez AIO, Lu H, Jiang HL, Zhang PX, Bruin B (2011) Mechanism of cobalt(II) porphyrin-catalyzed C-H amination with organic azides: radical nature and H-atom abstraction ability of the key cobalt(III)-nitrene intermediates. J Am Chem Soc 133:12264–12273. doi:10.1021/ja204800a
37. Tang H, Shen CY, Lin MR, Sen A (2000) Cobalt porphyrin-catalyzed alkane oxidations using dioxygen as oxidant. Inorg Chim Acta 300:1109–1111. doi:10.1016/S0020-1693(99)00572-1
38. Menon CC, Kapur SL (1961) A new redox system for vinyl polymerization in aqueous medium. J Polym Sci 54:45–51. doi:10.1002/pol.1961.1205415904
39. Sun Y, Zhai GQ (2013) CuSO4-catalyzed self-initiated radical polymerization of 2-(*N*, *N*-dimethylamino)ethyl methacrylate as an intrinsically reducing inimer. Chin J Polym Sci 31:1161–1172. doi:10.1007/s10118-013-1317-5
40. Wang F, Sayre LM (1992) Kinetics and mechanism of aliphatic amine oxidation by aqueous $(batho)_2Cu(II)$. J Am Chem Soc 114:248–255. doi:10.1021/ja00027a032
41. Wang F, Sayre LM (1989) Oxidation of tertiary amine buffers by copper (II). Inorg Chem 28:169–170. doi:10.1021/ic00301a001
42. Moffett JW, Zika RG (1987) Reaction kinetics of hydrogen peroxide with copper and iron in seawater. Environ Sci Technol 21:804–810. doi:10.1021/es00162a012
43. Brenner AJ, Harris ED (1995) A quantitative test for copper using bicinchoninic acid. Anal Biochem 226:80–84. doi:10.1006/abio.1995.1194
44. Karlin KD, Wei N, Jung B et al (1993) Kinetics and thermodynamics of formation of copper–dioxygen adducts: oxygenation of mononuclear copper (I) complexes containing tripodal tetradentate ligands. J Am Chem Soc 115:9506–9514. doi:10.1021/ja00074a015
45. Machonkin TE, Zhang HH, Hedman B et al (1998) Spectroscopic and magnetic studies of human ceruloplasmin: identification of a redox-inactive reduced type 1 copper site. Biochemistry 37:9570–9578. doi:10.1021/bi980434v
46. Huang JB (ed) (2002) Industrial gas manual. Chemical Industry Press, Beijing
47. Pantoustier N, Moins S, Wautier M, Degée P, Dubois P (2003) Solvent-free synthesis and purification of poly [2-(dimethylamino) ethyl methacrylate] by atom transfer radical polymerization. Chem Commun 3:340–341. doi:10.1039/B208703K

48. Giz A, Catalgil-Giz H, Alb A, Brousseau JL, Reed WF (2001) Kinetics and mechanisms of acrylamide polymerization from absolute, online monitoring of polymerization reaction. Macromolecules 34:1180–1191. doi:10.1021/ma000815s
49. Hunkeler D (1991) Mechanism and kinetics of the persulfate-initiated polymerization of acrylamide. Macromolecules 24:2160–2171. doi:10.1021/ma00009a004
50. Cai ZQI, Wang WC, Ruan G, Wen XF (2012) Kinetic study of acrylamide radical polymerization initiated by the horseradish peroxidase-mediated system. Int J Chem Kinet 44:475–481. doi:10.1002/kin.20611
51. Fuxman AM, McAuley KB, Schreiner LJ (2003) Modeling of free-radical crosslinking copolymerization of acrylamide and *N*, *N*′-methylenebis(acrylamide) for radiation dosimetry. Macromol Theory Simul 12:647–662. doi:10.1002/mats.200350050
52. Rieger J, Zhang W, Stoffelbach F, Charleux B (2010) Surfactant-free RAFT emulsion polymerization using poly (*N*, *N*-dimethylacrylamide) trithiocarbonate macromolecular chain transfer agents. Macromolecules 43:6302–6310. doi:10.1021/ma1009269
53. Tang HD, Radosz M, Shen YQ (2006) CuBr 2/N, *N*, *N*′, *N*′-Tetra [(2-pyridal) methyl] ethylenediamine/tertiary amine as a highly active and versatile catalyst for atom-transfer radical polymerization via activator generated by electron transfer. Macromol Rapid Commun 27:1127–1131. doi:10.1002/marc.200600258
54. Kwak Y, Matyjaszewski K (2009) ARGET ATRP of methyl methacrylate in the presence of nitrogen-based ligands as reducing agents. Polym Int 58:242–247. doi:10.1002/pi.2530
55. Nelsen SF, Ippoliti JT (1986) The deprotonation of trialkylamine cation radicals by amines. J Am Chem Soc 108:4879–4881. doi:10.1021/ja00276a028
56. Weiss JF, Tollin G, Yoke JT (1964) Reactions of triethylamine with copper halides. II. Internal oxidation-reduction of dichlorobis (triethylamine) copper (II). Inorg Chem 3:1344–1348. doi:10.1021/ic50020a002
57. Mahapatra S, Halfen JA, Tolman WB (1996) Mechanistic study of the oxidative *N*-dealkylation reactions of Bis (μ-oxo) dicopper complexes. J Am Chem Soc 118:11575–11586. doi:10.1021/ja962304k
58. Kanoufi F, Zu Y, Bard AJ (2001) Homogeneous oxidation of trialkylamines by metal complexes and its impact on electrogenerated chemiluminescence in the trialkylamine/Ru $(bpy)_3^{2+}$ system. J Phys Chem B 105:210–216. doi:10.1021/jp002880
59. Wayner DDM, Clark KB, Rauk A, Yu D, Armstrong DA (1997) C-H bond dissociation energies of alkyl amines: radical structures and stabilization energies. J Am Chem Soc 119:8925–8932. doi:10.1021/ja971365v
60. Tang H, Shen Y, Li BG et al (2008) Tertiary amine-enhanced activity of ATRP catalysts CuBr/TPMA and CuBr/Me6TREN. Macro Rapid Commun 29:1834–1838. doi:10.1002/marc.200800378
61. Tang H, Radosz M, Shen Y (2006) CuBr 2/N, *N*, *N*′, *N*′-Tetra[(2-pyridal)methyl] ethylenediamine/tertiary amine as a highly active and versatile catalyst for atom-transfer radical polymerization via activator generated by electron transfer. Macro Rapid Commun 27:1127–1131. doi:10.1002/marc.200600258
62. Dong HC, Matyjaszewski K (2008) ARGET ATRP of 2-(dimethylamino)ethyl methacrylate as an intrinsic reducing agent. Macromolecules 41:6868–6870. doi:10.1021/ma8017553
63. Coullerez G, Malmström E, Jonsson M (2006) Solvent effects on the redox properties of Cu complexes used as mediators in atom transfer radical polymerization. J Phys Chem A 110:10355–10360. doi:10.1021/jp057191i
64. Bortolamei N, Isse AA, Di Marco VB, Gennaro A, Matyjaszewsk K (2010) Thermodynamic properties of copper complexes used as catalysts in atom transfer radical polymerization. Macromolecules 43:9257–9267. doi:10.1021/ma101979p
65. Tang H, Shen C, Lin M, Sen A (2000) Cobalt porphyrin-catalyzed alkane oxidations using dioxygen as oxidant. Inorg Chim A 300:1109–1111. doi:10.1016/S0020-1693(99)00572-1
66. Taki M, Itoh S, Fukuzumi S (2002) Oxo-transfer reaction from a bis (μ-oxo) dicopper (III) complex to sulfides. J Am Chem Soc 124:998–1002. doi:10.1021/ja016023a
67. Mizuno M, Hayashi H, Fujinami S et al (2003) Ligand effect on reversible conversion between copper (i) and bis (μ-oxo) dicopper (iii) complex with a sterically hindered tetradentate tripodal ligand and monooxygenase activity of bis (μ-oxo) dicopper (iii) complex. Inorg Chem 42:8534–8544. doi:10.1021/ic0345166

68. Spencer DJE, Reynolds AM, Holland PL et al (2002) Copper chemistry of β-diketiminate ligands: monomer/dimer equilibria and a new class of bis (μ-oxo) dicopper compounds. Inorg Chem 41:6307–6321. doi:10.1021/ja016023a
69. Meunier B, Bernadou J (2002) Metal-oxo species in P450 enzymes and biomimetic models. Oxo-hydroxo tautomerism with water-soluble metalloporphyrins. Top Catal 21:47–54
70. Norman RE, Yan S, Que L Jr et al (1990) (μ-Oxo)(μ-carboxylato) diiron (III) complexes with distinct iron sites. Consequences of the inequivalence and its relevance to dinuclear iron-oxo proteins. J Am Chem Soc 112:1554–1562. doi:10.1021/ja00160a039
71. Quinonero D, Morokuma K, Musaev DG et al (2005) Metal-peroxo versus metal-oxo oxidants in non-heme iron-catalyzed olefin oxidations: computational and experimental studies on the effect of water. J Am Chem Soc 127:6548–6549. doi:10.1021/ja051062y
72. Kumar K, Endicott JF (1984) Oxidation–reduction reactions of complexes with macrocyclic ligands. Electron-transfer reactivity of a 1:1 cobalt(II)-dioxygen adduct. Inorg Chem 23:2447–2452. doi:10.1021/ic00184a018
73. Mattioli G, Giannozzi P, Amore Bonapasta A et al (2013) Reaction pathways for oxygen evolution promoted by cobalt catalyst. J Am Chem Soc 135:15353–15363. doi:10.1021/ja401797v
74. Ishida T, Kondo S, Tsuda K (1997) Free-radical polymerization of methyl methacrylate initiated by *N*, *N*-dimethylaniline. Makromol Chem 178:3221–3228. doi:10.1002/macp.1977.021781207
75. Tsuda K, Kondo S, Yamashita K, Ito K (1984) Initiation mechanism of free-radical polymerization of methyl methacrylate by *p*-substituted *N*, *N*-dimethylanilines. Makromol Chem 185:81–89. doi:10.1002/macp.1984.021850109